Protonated High Energy Density Materials: N_4 Tetrahedron and N_8 Octahedron

Matthew L. Leininger,† Timothy J. Van Huis,‡ and Henry F. Schaefer III*

Center for Computational Quantum Chemistry, University of Georgia, Athens, Georgia 30602

Received: January 17, 1997; In Final Form: March 26, 1997[⊗]

Previous theoretical studies have demonstrated that tetrahedral N_4 should be an extraordinarily effective high energy density material. But this species has thus far resisted laboratory efforts directed to its synthesis. *Ab initio* electronic structure methods have been used to examine the T_d N_4 and O_h N_8 nitrogen clusters, including their protonated forms. We have optimized geometries using DZP, TZ2P, and TZ2P(f,d) basis sets with the Hartree−Fock self-consistent-field (SCF) method, second-order Møller−Plesset perturbation theory (MP2), single and double excitation configuration interaction (CISD), coupled-cluster (CCSD and CCSD(T)) methods, and three DFT/Hartree−Fock hybrid (B3LYP, B3P86, BHLYP) methods. Harmonic vibrational frequencies and infrared intensities have been obtained at the SCF, MP2, B3LYP, B3P86, and BHLYP levels of theory. The vertex protonated O_h N_8 and T_d N_4 structures are found to represent minima on their respective potential energy surfaces. The bond protonated T_d N_4 molecule was determined to be a transition state leading to the vertex protonated T_d N_4 isomer. The predicted proton affinities of T_d N_4 and O_h N_8 support the possibility that standard laboratory techniques for deprotonation may be used to yield these elusive high-energy density materials. The molecular properties determined at the DFT/Hartree−Fock hybrid level of theory are compared to large basis set coupled-cluster results and found to be in good agreement, even when relatively small basis sets are used for the former.

I. Introduction

The characterization and development of efficient and environmentally safe energy sources are of obvious technological significance. Several theoretical studies have identified the N_n ($n \geq 4$) systems as excellent high energy density material (HEDM) candidates. Bliznyuk, Shen, and Schaefer have shown that N_{20} has a metastable dodecahedral geometry analogous to the $C_{20}H_{20}$ dodecahedrane.[1] This structure lies 50 kcal/mol of nitrogen atoms above 10 N_2 molecules, making N_{20} a potential high energy density material. Other theoretical studies have focused on octaazacubane. Trinquier, Malrieu, and Dudley[2] used a pseudopotential SCF method to show that octaazacubane was higher in energy than two N_4 molecules. However, they could only assume that the optimized N_8 stationary point was a minimum on the potential energy surface. Octaazacubane was shown to be a minimum when Engelke and Stine[3] performed vibrational frequency calculations at the SCF level using several basis sets. Additionally, these authors showed N_8 to have a high activation barrier for decomposition to four N_2 molecules.

Engelke[4] and the group of Alkorta, Elguero, Rozas, and Balaban[5] have examined octaazacubane as part of the series $(CH)_{8-n}N_n$ where $0 \leq n \leq 8$. These studies indicated that the heat of formation of these compounds grows with increasing n and that the high-energy content of the polyazacubanes is due not to strain energy but to weak N−N single bonds. Lauderdale, Stanton, and Bartlett[6] were the first to optimize octaazacubane using correlated theoretical methods. Their results indicated that electron correlation has large effects on the equilibrium geometry and vibrational frequencies of octaazacubane. In addition, their research obtained estimates of the energy difference between N_8 and four N_2 by employing coupled-cluster methods including coupled-cluster singles and doubles (CCSD).[7] Using several correlated methods, Leininger, Sherrill, and Schaefer[8] have shown three N_8 isomers to represent minima on the N_8 potential energy surface. In order to yield a more reliable estimate of the energy difference $\Delta E(N_8 - 4N_2)$, 423 kcal/mol, they included a perturbative correction for triple excitations by utilizing the CCSD(T) method.[9] On the basis of the dissociation energies and specific impulse, the authors concluded that the high-energy content of the nitrogen species suggests that they represent better explosives or propellants than several oxygen HEDM candidates. Recently, Tian, Ding, Zhang, Xie, and Schaefer[10] have examined two new N_8 isomers which only have N−N single bonds and found them to be minima and lower lying than O_h octaazacubane by 47 and 72 kcal/mol, respectively.

The tetrahedral form of N_4 has been the focus on several theoretical studies which have led to an understanding of the structure and energetics of the T_d N_4 potential energy surface. Venanzi and Schulman[11] demonstrated that T_d N_4 is a minimum on the DZ SCF potential energy surface. Francl and Chesick[12] were the first to optimize T_d N_4 using correlated methods. They found that perturbation theory is inadequate for an accurate description of T_d N_4. Lee and Rice,[13] using the CCSD(T) method, estimated the barrier separating T_d $N_4(^1A_1)$ from two N_2 molecules to be 61 kcal/mol, while the estimated energy difference $\Delta E(N_4 - 2N_2)$ was 186 kcal/mol, thus indicating that T_d N_4 is a metastable species which, if synthesized, should have a reasonably long lifetime. To confirm the stability of the $^1A_1$ state, the authors also explored the $^3A''$ state near the T_d N_4 equilibrium region of the PES and found it to lie 13 kcal/mol above the $^1A_1$ state. Lauderdale et al.[6] found a T_d N_4 minimum on the CCSD potential energy surface and investigated several reaction pathways to other N_4 structures. Glukhovtsev and Schleyer[14] examined numerous N_4 structures and found the lowest-energy conformation to be a C_{2h} open-chain triplet structure. Using multiconfigurational wave functions, Dunn and Morokuma[15] estimated the N_4 dissociation barrier to be 63 kcal/mol, surprisingly close to the value reported by Lee and Rice.[13] Yarkony[16] has considered the spin-forbidden radiationless decay

* To whom correspondence should be addressed.
† Samuel Francis Boys Graduate Fellow.
‡ Abraham Baldwin Graduate Fellow.
⊗ Abstract published in *Advance ACS Abstracts,* May 15, 1997.

S1089-5639(97)00258-2 CCC: $14.00 © 1997 American Chemical Society

of T_d N_4 and found the energy difference between the minimum-energy crossing structure and the energy at the minimum on the bound state PES to be 28 kcal/mol, or half the barrier for the spin-allowed decay channel. Hence, the lowest-lying vibrational levels of T_d N_4 should not dissociate via the spin-forbidden triplet pathway.

Pointing toward the laboratory synthesis of these species, we extend the theoretical consideration of octaazacubane and T_d N_4 to include their protonated forms. Using DZP, TZ2P, and TZ2P(f,d) basis sets, we report optimized geometries and harmonic vibrational frequencies for octaazacubane (**1**), vertex protonated N_8 (**2**), T_d N_4 (**3**), vertex protonated T_d N_4 (**4**), and bond protonated T_d N_4 (**5**). Of the protonated species, we find **2** and **4** to represent minima on their respective potential energy surfaces, while **5** is the transition state leading to the vertex protonated structure (**4**). The proton affinities of T_d N_4 and O_h N_8 are also reported, as these quantities are essential if a reaction path is to be developed to yield the protonated form of T_d N_4 or octaazacubane. Standard experimental techniques for deprotonation might then be utilized to yield these, to date, elusive HEDM clusters.

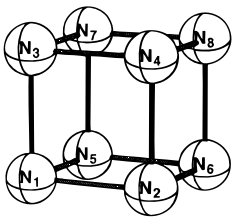

(1)

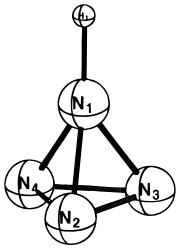

(4)

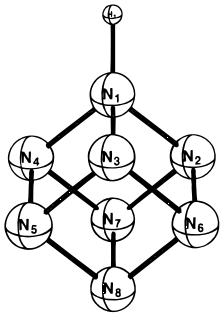

(2)

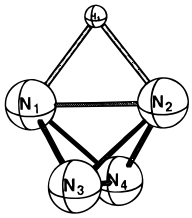

(5)

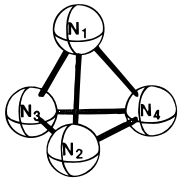

(3)

II. Theoretical Methods

Three basis sets of contracted Gaussian functions were employed in the present study. Our double-ζ plus polarization (DZP) basis is the standard Huzinaga−Dunning[17,18] double-ζ (9s5p) augmented with a set of six Cartesian d-type polarization functions on each nitrogen atom [$\alpha_d(N) = 0.80$] and a set of p-type functions on hydrogen [$\alpha_p(H) = 0.70$]. The triple-ζ plus double polarization (TZ2P) basis consists of Huzinaga's[17] (10s6p) primitive set for nitrogen and (5s) primitive set for hydrogen contracted by Dunning[19] to (5s3p) for nitrogen and (3s) for hydrogen and is augmented with two sets of six Cartesian d-type polarization functions for nitrogen [$\alpha_d(N) = 1.60, 0.40$] and two sets of p-type functions on hydrogen [$\alpha_p(H) = 1.50, 0.375$]. The TZ2P(f,d) basis set was the largest used in this study, and it consisted of a set of 10 Cartesian f-like functions added to the described TZ2P basis for nitrogen, [$\alpha_f(N) = 1.00$], and a set of six Cartesian d-like functions added for the hydrogen, [$\alpha_d(H) = 1.00$]. With a DZP basis set, the deprotonated N_4 species consisted of 64 contracted Gaussian basis functions. The protonated N_4 species, **4** and **5**, contained 69 contracted Gaussian functions. Similarly, the DZP basis set yields 128 contracted Gaussian basis functions for the deprotonated N_8 species, **1**, and 133 functions for the protonated form, **2**. The TZ2P basis consisted of 104 and 113 basis functions, and the TZ2P(f,d) basis 144 and 159 contracted basis functions for the deprotonated and protonated N_4 species, respectively. The theoretical methods employed are restricted Hartree−Fock (RHF), second-order Møller−Plesset perturbation theory (MP2), single and double excitation configuration interaction (CISD),[20,21] and coupled-cluster (CCSD)[7,22] and several hybrid Hartree−Fock/DFT methods. Three different gradient corrected exchange-correlation (XC) functionals were employed: B3LYP, BHLYP, and B3P86. The first two utilize the correlation functional of Lee, Yang, and Parr (LYP)[23] while the third used that of Perdew (P86).[24] Becke's three-parameter[25] (B3) and approximate[26] half-and-half[27] (BH) Hartree−Fock hybrid treatments were combined with the different correlation functionals to form the three XC functionals. For the CI wave functions, the contribution of unlinked quadruple excitations is estimated by Davidson's formula.[28] For coupled-cluster wave functions, the additional effect of connected triple excitations was estimated perturbatively according to the CCSD(T) method.[9,29]

Geometries were optimized using analytic first derivatives at the SCF,[30] MP2,[31] CISD,[32,33] CCSD,[34] CCSD(T),[35] and Hartree−Fock/DFT hybrid levels of theory. Harmonic vibrational frequencies were determined analytically for SCF[31,36] and Hartree−Fock/DFT hybrid methods or by finite differences of the analytic first derivatives at the MP2 level. Infrared intensities were determined analytically at the SCF[37] and DFT levels, while the MP2 infrared intensities were evaluated via finite differences of dipole moments. For the CI and coupled-cluster methods, the core orbitals (N 1s-like) were constrained to be doubly occupied, and the corresponding virtual orbitals were deleted from the correlation procedures. The wave functions for **1** and **3**, and **5** were obtained under C_{2v} symmetry, while **2** and **4** were obtained under C_s symmetry. For the CISD wave functions with a DZP basis there were 424 637 configuration state functions (CSF's) for **1** and 946 873 CSF's for **2**, 27 069 CSF's for **3**, 66 042 CSF's for **4**, 33 402 CSF's for **5**. With the TZ2P basis there were 94 153 CSF's for **3**, 228 382 CSF's for **4**, and 115 332 CSF's for **5**. The PSI *ab initio* programs[38] were used in the present study. MP2 results were obtained using the Cambridge Analytic Derivatives Package (CADPAC)[39] while the Hartree−Fock/DFT hybrid results were obtained using the Gaussian94[26] suite of programs.

III. Results and Discussion

A. N_8. Total energies and optimized geometries at several levels of theory are presented in Table 1 and 2. For small molecules at their equilibrium geometries it has been accepted that the DZP CISD and TZ2P CCSD methods typically provide very balanced predictions of equilibrium geometries.[40−42] Since CISD is not size extensive, its treatment of electron correlation is likely to be less complete in the study of the larger N_8 and protonated N_8 structures, leading to relatively shorter theoretical bond lengths. We therefore anticipate the true equilibrium bond

TABLE 1: Total Energies (hartrees) and Proton Affinities (kcal/mol) in Parentheses for N_8H^+

basis and theory	N_8	vertex	basis and theory	N_8	vertex
DZP SCF	−435.054 757	(168.3)	DZP BHLYP	−437.251 560	(166.8)
DZP MP2	−436.464 235	(166.4)	DZP CISD	−436.055 002	(169.3)
DZP B3LYP	−437.520 976	(168.0)	DZP CISD+Q[a]	−436.258 123	(169.4)
DZP B3P86	−438.527 458	(168.1)	DZP CCSD	−436.375 146	(169.7)

[a] At DZP CISD optimized geometry, ref 8.

TABLE 2: Geometrical Parameters Including Bond Length (Å) for N_8 and N_8H^+

	N_8	vertex protonated N_8				
basis and theory	r_{NN}	r_{NH}	r_{13}	r_{45}	r_{47}	r_{78}
DZP SCF	1.461	1.022	1.452	1.469	1.469	1.462
DZP MP2	1.529	1.042	1.494	1.556	1.556	1.527
DZP B3LYP	1.517	1.042	1.495	1.537	1.536	1.517
DZP B3P86	1.504	1.040	1.481	1.523	1.522	1.504
DZP BHLYP	1.484	1.031	1.469	1.496	1.496	1.484
DZP CISD	1.479	1.027	1.464	1.491	1.491	1.480
DZP CCSD	1.517	1.038	1.492	1.536	1.536	1.518

TABLE 3: Harmonic Vibrational Frequencies (cm^{-1}) and IR Intensities (km/mol, in Parentheses) for O_h Symmetry Octaazacubane, N_8[a]

	DZP				
mode	SCF	MP2	B3LYP	B3P86	BHLYP
A_{2u}	1356	1078	1137	1147	1243
E_g	1265	1016	1060	1097	1166
T_{2u}	1182	893	956	993	1071
A_{1g}	1175	886	949	984	1070
T_{2g}	1107	808	868	887	979
T_{1u}	1091 (3)	748 (7)	822 (7)	859 (8)	962 (5)
T_{2g}	983	674	759	786	880
E_u	735	464	529	530	628

[a] T_{1u} is the only IR-active mode.

lengths to lie somewhere between those determined at the DZP CISD and DZP CCSD levels of theory.

The N−N bond length in octaazacubane at the DZP SCF level of theory is 1.461 Å and increases 0.056, 0.043, and 0.023 Å using B3LYP, B3P86, and BHLYP, respectively. Each Hartree−Fock/DFT hybrid method yields equilibrium bond lengths between the CISD and CCSD levels of theory, with B3LYP best approximating the CCSD results. As previously reported in the literature,[8] MP2 significantly overestimates the effects of correlation, producing a bond length of 1.529 or 0.012 Å larger than the CCSD results. The CISD and CCSD bond lengths are slightly longer than the typical N−N single bond (1.449 Å).[43] In most cases, the theoretical geometries for structures **1** and **2** demonstrate the same general trends in the effect of correlation on equilibrium bond lengths. The bond lengths are predicted according to r_e(SCF) < r_e(CISD) < r_e(BHLYP) < r_e(B3P86) < r_e(CCSD) < r_e(B3LYP), with the correlated bond distances typically longer than the SCF results by 0.01−0.04 Å for CISD and BHLYP, 0.02−0.06 Å for B3P86, and 0.02−0.07 Å for CCSD and B3LYP. The same general trend holds true for the predicted N−H bond length in the vertex protonated ocaazacubane, which is slightly longer than the typical N−H bond (1.012 Å).[43]

The theoretical harmonic vibrational frequencies and IR intensities for octaazacubane, (**1**) and vertex protonated octaazacubane (**2**) at the SCF, MP2, B3LYP, B3P86, and BHLYP level are given in Tables 3 and 4. The vertex protonated structure was predicted to be a minimum on the N_8H^+ potential energy surface (PES). Correlation has a large effect on the harmonic vibrational frequencies, as evidenced by the 4−35% decrease in the frequencies for octaazacubane and its vertex protonated form. This large decrease can be attributed to the long N−N bonds at the MP2 level. The vertex protonated N_8 exhibits a relatively strong IR intensity, which corresponds to the N−H stretching mode. The bond and face protonated forms of octaazacubane were determined to represent higher order stationary points on their respective potential energy surfaces, with two and three imaginary frequencies, and therefore were not considered for further study. An MO Hessian analysis[44] of all N_8 species revealed the SCF wave function to be stable with respect to rotation of the molecular orbitals.

TABLE 4: Harmonic Vibrational Frequencies (cm^{-1}) and IR Intensities (km/mol, in Parentheses) for the Vertex Protonated Species N_8H^+

mode	SCF	MP2	B3LYP	B3P86	BHLYP
A_1	3586 (287)	3340 (210)	3307 (198)	3329 (197)	3444 (251)
E	1456 (63)	1272 (55)	1262 (58)	1282 (59)	1348 (61)
A_1	1345 (1)	1073 (1)	1127 (<1)	1140 (<1)	1233 (<1)
E	1240 (<1)	1002 (<1)	1028 (<1)	1065 (<1)	1136 (<1)
A_2	1163 (0)	841 (0)	913 (0)	970 (<1)	1051 (<1)
A_1	1157 (3)	895 (3)	934 (<1)	950 (<1)	1040 (<1)
E	1155 (<1)	899 (<1)	930 (<1)	964 (<1)	1039 (<1)
A_1	1104 (<1)	817 (1)	879 (1)	903 (3)	987 (1)
A_1	1069 (6)	762 (22)	808 (16)	841 (16)	942 (10)
E	1064 (4)	800 (<1)	840 (<1)	859 (<1)	932 (<1)
E	1015 (<1)	685 (7)	718 (<1)	798 (9)	914 (5)
A_1	958 (8)	629 (3)	705 (3)	732 (4)	842 (7)
E	928 (1)	659 (2)	763 (9)	746 (<1)	833 (<1)
E	733 (6)	479 (8)	531 (6)	534 (7)	628 (6)

TABLE 5: Total Energies (hartrees) and Proton Affinities (kcal/mol) for N_4 and N_4H^+

basis and theory	N_4	vertex	bond
DZP SCF	−217.579 501	(139.8)	(108.7)
DZP MP2	−218.317 295	(137.1)	(119.0)
DZP CISD	−218.150 094	(141.2)	(114.7)
DZP CISD+Q[a]	−218.234 493	(141.6)	(117.1)
DZP CCSD	−218.248 384	(141.8)	(118.1)
DZP CCSD(T)	−218.281 690	(141.8)	(121.1)
DZP B3LYP	−218.815 467	(140.7)	(117.5)
DZP BHLYP	−218.673 827	(139.5)	(112.7)
DZP B3P86	−219.319 806	(141.0)	(117.6)
TZ2P SCF	−217.601 326	(142.1)	(111.0)
TZ2P MP2	−218.432 173	(137.8)	(117.7)
TZ2P CISD	−218.228 706	(142.7)	(114.6)
TZ2P CISD+Q[a]	−218.321 442	(142.7)	(116.6)
TZ2P CCSD	−218.336 958	(142.7)	(117.5)
TZ2P CCSD(T)	−218.384 229	(142.2)	(120.3)
TZ2P B3LYP	−218.842 214	(141.2)	(116.9)
TZ2P BHLYP	−218.696 884	(140.8)	(113.1)
TZ2P B3P86	−219.343 442	(142.1)	(118.1)
TZ2Pf SCF	−217.616 217	(142.3)	(110.5)
TZ2Pf CCSD	−218.441 446	(141.5)	(116.4)
TZ2Pf CCSD(T)	−218.465 116	(140.9)	(119.1)
TZ2Pf B3LYP	−218.852 390	(141.2)	(116.5)
TZ2Pf BHLYP	−218.709 095	(140.8)	(112.7)
TZ2Pf B3P86	−219.354 245	(142.1)	(117.7)

[a] At CISD optimized geometry.

B. N_4. The general geometry trends found in **1** and **2** continue in T_d N_4 and its protonated forms. Total energies and optimized geometries using several basis sets and levels of theory are reported in Tables 5 and 6. For each basis set used in this study, the BHLYP and CISD bond lengths are in good agreement, while the B3LYP method yields geometries comparable to the CCSD results. The most significant difference between CCSD and B3LYP, 0.014 Å, occurs in the N−H bond length of **5**, where the CCSD and B3LYP bond distances are 1.273 and 1.287 Å, respectively. With most of the methods used here, the predicted N−N bond lengths in the N_4 species are a bit shorter than a typical N−N single bond. However, at the highest level of theory and basis set most N−N bond lengths

TABLE 6: Bond Distances (Å) for N_4 and N_4H^+

basis and theory	N_4	bond				vertex		
	r_{NN}	r_{NH}	r_{12}	r_{13}	r_{34}	r_{NH}	r_{12}	r_{23}
DZP SCF	1.398	1.261	1.576	1.392	1.417	1.022	1.379	1.413
DZP MP2	1.484	1.280	1.660	1.474	1.539	1.039	1.434	1.536
DZP B3LYP	1.459	1.287	1.642	1.452	1.495	1.039	1.426	1.491
DZP B3P86	1.448	1.279	1.623	1.440	1.483	1.037	1.415	1.477
DZP BHLYP	1.426	1.272	1.605	1.419	1.455	1.030	1.400	1.449
DZP CISD	1.431	1.264	1.608	1.423	1.459	1.028	1.403	1.456
DZP CCSD	1.458	1.273	1.641	1.449	1.491	1.035	1.425	1.490
DZP CCSD(T)	1.472	1.279	1.661	1.464	1.511	1.037	1.435	1.511
TZ2P SCF	1.397	1.265	1.583	1.394	1.420	1.014	1.375	1.416
TZ2P MP2	1.489	1.280	1.669	1.479	1.548	1.029	1.429	1.548
TZ2P B3LYP	1.454	1.287	1.644	1.449	1.492	1.029	1.417	1.489
TZ2P B3P86	1.444	1.280	1.628	1.439	1.483	1.028	1.409	1.478
TZ2P BHLYP	1.422	1.273	1.608	1.418	1.454	1.020	1.393	1.448
TZ2P CISD	1.427	1.265	1.611	1.422	1.459	1.017	1.396	1.456
TZ2P CCSD	1.456	1.275	1.647	1.451	1.493	1.024	1.418	1.494
TZ2P CCSD(T)	1.476	1.282	1.672	1.471	1.519	1.026	1.432	1.522
TZ2Pf SCF	1.392	1.264	1.574	1.389	1.415	1.015	1.371	1.410
TZ2Pf B3LYP	1.448	1.286	1.636	1.443	1.485	1.031	1.413	1.481
TZ2Pf B3P86	1.438	1.280	1.619	1.433	1.476	1.029	1.404	1.470
TZ2Pf BHLYP	1.417	1.272	1.600	1.412	1.448	1.022	1.388	1.442
TZ2Pf CCSD	1.444	1.274	1.630	1.438	1.480	1.026	1.409	1.477
TZ2Pf CCSD(T)	1.463	1.282	1.653	1.458	1.504	1.028	1.422	1.503

are longer than a typical N−N single bond by 0.02−0.2 Å. The largest difference arises in **5** where the r_{12} has an elongated bond length which is 0.2 Å larger than a typical N−N single bond. The only exception to N−N bond distances longer than a typical N−N single bond is the r_{12} N−N bond in **4**, which is only 0.03 Å shorter than a typical N−N single bond. The N−N bond lengths are predicted according to r_e(SCF) < r_e(BHLYP) < r_e(CISD) < r_e(B3P86) < r_e(CCSD) < r_e(B3LYP) < r_e(CCSD(T)). The predicted bond lengths are typically longer than the SCF values by 0.03 Å for BHLYP and CISD, 0.01−0.06 Å for B3P86, 0.02−0.07 Å for CCSD and B3LYP, and 0.02−0.09 Å for CCSD(T).

The configuration interaction and coupled-cluster methods appear to be more sensitive to the basis set size relative to the DFT/Hartree−Fock hybrid methods, as evidenced by the fairly large change in geometry between CCSD and CCSD(T). This fact is particularly noticeable when f- and d-type functions are added to the TZ2P basis on the nitrogen and hydrogen atoms, respectively. The importance of connected triple excitations is evident from the CCSD(T) results. The equilibrium bond lengths increase an average of 0.015 Å from the CCSD to CCSD(T) levels of theory. As concluded by Lee and Rice,[13] we find the inclusion of the connected triple excitations to be more important than the addition of higher order angular momentum basis functions. For this study, TZ2P(f,d) CCSD(T) represents the highest level of theory which includes a balanced treatment of basis set and correlation effects. Surprisingly, the DZP B3LYP results show reasonable agreement with the geometries predicted at the TZ2P(f,d) CCSD(T) level of theory. However, as the basis set size increases, the B3LYP results converge upon the CCSD geometries rather than the CCSD(T) results. This conclusion is reinforced when comparing the B3LYP results with the coupled-cluster results of Lee et al.[13] They obtained optimized geometries and harmonic vibrational frequencies for N_4 at the CCSD and CCSD(T) levels of theory using large atomic natural orbital (ANO) basis sets. The DZP B3LYP predicted geometries again show a very reasonable agreement with the largest ANO, [4s3p2d1f], CCSD(T) results of Lee and Rice.[13] However, the harmonic vibrational frequencies predicted at the DZP B3LYP level of theory are of CCSD quality. Increasing the size of the basis set for B3LYP only serves to cause larger differences between the B3LYP and the large ANO, [5s4p3d2f], CCSD results.[13]

TABLE 7: Harmonic Vibrational Frequencies (cm^{-1}) and IR Intensities (km/mol, in Parentheses) for the N_4 Tetrahedron[a]

	DZP				
mode	SCF	MP2	B3LYP	B3P86	BHLYP
A_1	1672	1222	1384	1430	1524
T_1	1191 (15)	883 (2)	984 (5)	1029 (4)	1084 (8)
E	886	693	759	798	820

[a] T_1 is the only IR-active mode.

TABLE 8: Harmonic Vibrational Frequencies (cm^{-1}) and IR Intensities (km/mol, in Parentheses) for the Vertex Protonated Species N_4H^+

	DZP				
mode	SCF	MP2	B3LYP	B3P86	BHLYP
A_1	3598 (750)	3408 (615)	3386 (632)	3417 (636)	3491 (697)
A_1	1662 (9)	1285 (5)	1394 (9)	1439 (8)	1524 (9)
E	1278 (6)	983 (22)	1063 (15)	1104 (13)	1163 (11)
A_1	1202 (14)	828 (<1)	984 (3)	1028 (3)	1091 (6)
E	910 (8)	824 (48)	797 (24)	823 (17)	851 (17)
E	815 (88)	602 (18)	677 (54)	701 (64)	741 (69)

TABLE 9: Harmonic Vibrational Frequencies (cm^{-1}) and IR Intensities (km/mol, in Parentheses) for the Bond Protonated Species N_4H^+

	DZP				
mode	SCF	MP2	B3LYP	B3P86	BHLYP
B_2	1414i (5)	1038i (141)	1270i (13)	1219i (16)	1325i (4)
A_1	2389 (286)	2230 (209)	2175 (199)	2224 (207)	2288 (246)
A_1	1617 (8)	1168 (3)	1324 (7)	1373 (7)	1465 (8)
B_1	1270 (39)	1102 (41)	1117 (40)	1132 (35)	1184 (42)
B_1	1196 (20)	904 (10)	976 (10)	1020 (14)	1084 (13)
B_2	1153 (9)	953 (<1)	934 (5)	983 (5)	1037 (7)
A_1	1068 (10)	868 (9)	965 (2)	986 (2)	1013 (4)
A_1	961 (4)	723 (<1)	803 (1)	840 (<1)	877 (2)
A_2	757 (0)	620 (0)	669 (0)	717 (0)	710 (0)

The theoretical harmonic vibrational frequencies and IR intensities for N_4 and its protonated forms are reported in Tables 7−9 for the DZP basis set at the SCF, MP2, B3LYP, B3P86, and BHLYP levels of theory. The vertex protonated structure (**4**) was determined to be a minimum, while the bond protonated structure (**5**) represented a transition state on the N_4H^+ PES. Following the imaginary vibrational mode in **5** led to **4**. The predicted harmonic vibrational frequencies decrease from the SCF results by 17% for B3LYP, 14% for B3P86, and 8% for BHLYP. An N_4H^+ structure in which the proton is located on a face of T_d N_4 was investigated and determined to represent a higher order stationary point with three imaginary frequencies and therefore not considered for further study.

C. Proton Affinities. The theoretical proton affinities are shown in Tables 1 and 5. The most reliable results for the proton affinities of N_8H^+ and N_4H^+ are 170 and 141 kcal/mol, respectively. Many standard deprotonating agents have proton affinities greater than 200 kcal/mol.[43] Thus, standard techniques for deprotonation could possibly be used to produce these nitrogen clusters if a reaction path could be developed to yield their protonated forms. Further studies involving the effects of particular deprotonating agents on the nitrogen clusters would prove valuable. For protonated T_d N_4, the B3LYP method yields energy differences comparable to the CCSD results with each basis set used in this study. The DZP B3LYP and B3P86 energy differences approximate those predicted with TZ2P(f,d) CCSD(T) to better than 2 kcal/mol.

The difference in the proton affinities of these nitrogen clusters may be attributed to the orientation of proton attachment as well as how efficiently the cluster can redistribute the proton's

positive charge throughout the system. Interestingly, the vertex protonated species (**2** and **4**) exhibit a 29 kcal/mol difference in proton affinities even though both have the C_{3v} symmetry orientation of protonation. Examination of the Mulliken charges on the nitrogen clusters for the vertex protonated structures shows the N_4 cluster must support a larger positive charge on the nitrogen atoms than the analogous N_8 cluster. For **2** the largest positive charge on a nitrogen atom is 0.11, whereas for **4** it is 0.17. The C_{2v} protonated structure (**5**) displays a Mulliken charge of 0.13 on the bridging nitrogens and 0.18 on the opposing nitrogens.

IV. Conclusions

We have reported theoretical geometries, energies, infrared intensities, proton affinities, and harmonic vibrational frequencies for several protonated nitrogen clusters. The vertex protonated clusters (**2** and **4**) represent minima on the potential energy hypersurfaces at each level of theory used in this study. The bond protonated N_4 cluster is predicted to be a transition state between vertex protonated structures (**5**). The predicted proton affinities support the possibility that these protonated nitrogen clusters could be deprotonated with standard experimental techniques to yield these elusive high energy density materials. For these nitrogen clusters the performance of the Hartree−Fock/DFT hybrid methods is quite promising. These hybrid methods obtain reasonable predictions of the molecular properties studied here, at a greatly reduced computational expense. Our laboratory expects continued progress in the calibration of these Hartree−Fock/DFT hybrid methods to more challenging molecular systems.

Acknowledgment. The authors thank Drs. Horst Sulzbach and Peter Schreiner for helpful Gaussian advice. This material is based upon work supported by the Air Force Office of Scientific Research under Grant 95-1-0057.

References and Notes

(1) Bliznyuk, A. A.; Shen, M.; Schaefer, H. F. *Chem. Phys. Lett.* **1992**, *198*, 249.
(2) Trinquier, G.; Malrieu, J. P.; Daudey, J.-P. *Chem. Phys. Lett.* **1981**, *80*, 552.
(3) Engelke, R.; Stine, J. R. *J. Phys. Chem.* **1990**, *94*, 5689.
(4) Engelke, R. *J. Am. Chem. Soc.* **1993**, *115*, 2961.
(5) Alkorta, I.; Elguero, J.; Rozas, I.; Balaban, A. T. *J. Mol. Struct. (THEOCHEM)* **1990**, *206*, 67.
(6) Lauderdale, W. J.; Stanton, J. F.; Bartlett, R. J. *J. Phys. Chem.* **1992**, *96*, 1173.
(7) Purvis, G. D.; Bartlett, R. J. *J. Chem. Phys.* **1982**, *76*, 1910.
(8) Leininger, M. L.; Sherrill, C. D.; Schaefer, H. F. *J. Phys. Chem.* **1995**, *99*, 2324.
(9) Raghavachari, K.; Trucks, G. W.; Pople, J. A.; Head-Gordon, M. *Chem. Phys. Lett.* **1989**, *157*, 479.
(10) Tian, A.; Ding, F.; Zhang, L.; Xie, Y.; Schaefer, H. F. *J. Phys. Chem. A* **1997**, *101*, 1946.
(11) Venanzi, T. J.; Schulman, J. M. *Mol. Phys.* **1975**, *30*, 281.
(12) Francl, M. M.; Chesick, J. P. *J. Phys. Chem.* **1990**, *94*, 526.
(13) Lee, T. J.; Rice, J. E. *J. Chem. Phys.* **1991**, *94*, 1215.
(14) Glukhovtsev, M. N.; Schleyer, P. v. R. *Int. J. Quantum Chem.* **1193**, *46*, 119.
(15) Dunn, K. M.; Morokuma, K. *J. Chem. Phys.* **1995**, *102*, 4904.
(16) Yarkony, D. R. *J. Am. Chem. Soc.* **1992**, *114*, 5406.
(17) Huzinaga, S. *J. Chem. Phys.* **1965**, *42*, 1293.
(18) Dunning, T. H. *J. Chem. Phys.* **1970**, *53*, 2823.
(19) Dunning, T. H. *J. Chem. Phys.* **1971**, *55*, 716.
(20) Shavitt, I. *Int. J. Quantum Chem. Symp.* **1978**, *12*, 5.
(21) Brooks, B. R.; Schaefer, H. F. *J. Chem. Phys.* **1979**, *70*, 5092.
(22) Scuseria, G. E.; Scheiner, A. C.; Lee, T. J.; Rice, E.; Schaefer, H. F. *J. Chem. Phys.* **1987**, *86*, 2881.
(23) Lee, C.; Yang, W.; Parr, R. G. *Phys. Rev. B* **1988**, *37*, 785.
(24) Perdew, J. *Phys. Rev. B* **1986**, *34*, 7046.
(25) Becke, A. D. *J. Chem. Phys.* **1993**, *98*, 5648.
(26) Gaussian 94, Revision C.3: Frisch, M. J.; Trucks, G. W.; Schlegel, H. B.; Gill, P. M. W.; Johnson, B. G.; Robb, M. A.; Cheeseman, J. R.; Keith, T.; Petersson, G. A.; Montgomery, J. A.; Raghavachari, K.; Al-Laham, M. A.; Zakrzewski, V. G.; Ortiz, J. V.; Foresman, J. B.; Cioslowski, J.; Stefanov, B. B.; Nanayakkara, A.; Challacombe, M.; Peng, C. Y.; Ayala, P. Y.; Chen, W.; Wong, M. W.; Andres, J. L.; Replogle, E. S.; Gomperts, R.; Martin, R. L.; Fox, D. J.; Binkley, J. S.; Defrees, D. J.; Baker, J.; Stewart, J. P.; Head-Gordon, M.; Gonzalez, C.; Pople, J. A. Gaussian, Inc., Pittsburgh, PA, 1995.
(27) Becke, A. D. *J. Chem. Phys.* **1993**, *42*, 2193.
(28) Langhoff, S. R.; Davidson, E. R. *Int. J. Quantum Chem.* **1986**, *8*, 337.
(29) Scuseria, G. E.; Lee, T. J. *J. Chem. Phys.* **1990**, *93*, 5851.
(30) Pulay, P. *Mol. Phys.* **1969**, *17*, 197.
(31) Pople, J. A.; Krishnan, R.; Schlegel, H. B.; Binkley, J. S. *Int. J. Quantum Chem. Symp.* **1979**, *13*, 225.
(32) Brooks, B. R.; Laidig, W. D.; Saxe, P.; Goddard, J. D.; Yamaguchi, Y.; Schaefer, H. F. *J. Chem. Phys.* **1980**, *72*, 4652.
(33) Rice, J. E.; Amos, R. D.; Handy, N. C.; Lee, T. J.; Schaefer, H. F. *J. Chem. Phys.* **1986**, *85*, 963.
(34) Scheiner, A. C.; Scuseria, G. E.; Rice, J. E.; Lee, T. J.; Schaefer, H. F. *J. Chem. Phys.* **1987**, *87*, 5361.
(35) Scuseria, G. E. *J. Chem. Phys.* **1991**, *94*, 442.
(36) Osamura, Y.; Yamaguchi, Y.; Saxe, P.; Vincent, M. A.; Gaw, J. F.; Schaefer, H. F. *Chem. Phys.* **1982**, *72*, 131.
(37) Yamaguchi, Y.; Frisch, M. J.; Gaw, J. F.; Schaefer, H. F. *J. Chem. Phys.* **1986**, *84*, 2262.
(38) PSI 2.0.8: Janssen, C. L.; Seidl, E. T.; Scuseria, G. E.; Hamilton, T. P.; Yamaguchi, Y.; Remington, R. B.; Xie, Y.; Vacek, G.; Sherrill, C. D.; Crawford, T. D.; Fermann, J. T.; Allen, W. D.; Brooks, B. R.; Fitzgerald, G. B.; Fox, D. J.; Gaw, J. F.; Handy, N. C.; Laidig, W. D.; Lee, T. J.; Pitzer, R. M.; Rice, J. E.; Saxe, P.; Scheiner, A. C.; Schaefer, H. F. PSITECH, Inc., Watkinsville, GA 30677, 1995. This program is generally available for a handling fee of $100.
(39) CADPAC5, suite of quantum chemistry programs developed by R. D. Amos with contributions from: I. L. Alberts, A.; Andrews, J. S.; Colwell, S. M.; Handy, N. C.; Jayatilaka, D.; Knowles, P. J.; Kobayashi, R.; Koga, N.; Laidig, K. E.; Maslen, P. E.; Murray, C. W.; Rice, J. E.; Sanz, J.; Simandiras, E. D.; Stone, A. J.; Su, M.-D. The Cambridge Analytic Derivatives Package Issue 5, 1992.
(40) Thomas, J. R.; DeLeeuw, B. J.; Vacek, G.; Schaefer, H. F. *J. Chem. Phys.* **1993**, *98*, 1336.
(41) Thomas, J. R.; DeLeeuw, B. J.; Vacek, G.; Crawford, T. D.; Yamaguchi, Y.; Schaefer, H. F. *J. Chem. Phys.* **1993**, *99*, 403.
(42) Schaefer, H. F.; Thomas, J. R.; Yamaguchi, Y.; DeLeeuw, B. J.; Vacek, G. In *Modern Electronic Structure Theory Part I*; Yarkony, D. R., Ed.; World Scientific: Singapore, 1995; p 3.
(43) Hehre, W. J.; Radom, L.; Schleyer, P. v. R.; Pople, J. A. In *Ab Initio Molecular Orbital Theory*; Wiley: New York, 1986.
(44) Yamaguchi, Y.; Alberts, I. L.; Goddard, J. D.; Schaefer, H. F. *Chem. Phys.* **1990**, *147*, 309.